

arXiv.org: cond-mat/0103211

**A Superconductor Made by a Metal Heterostructure
at the Atomic Limit Tuned at the "Shape Resonance": MgB₂**

A. Bianconi*, D. Di Castro, S. Agrestini, G. Campi, N. L. Saini,
*Unit INFM and Dipartimento di Fisica, Universit di Roma "La Sapienza",
P. le Aldo Moro 2, 00185 Roma, Italy*

A. Saccone, S. De Negri, M. Giovannini
*Dipartimento di Chimica e Chimica Industriale, Universit di Genova,
Via Dodecaneso 31, 16146 Genova, Italy*

(received march 7, 2001)

We have studied the variation of T_c with charge density and lattice parameters in $Mg_{1-x}Al_xB_2$ superconducting samples at low Al doping $x < 8\%$. We show that high T_c occurs where the chemical potential is tuned at a superconducting shape resonance near the energy E_c of the quantum critical point (QCP) for the dimensional transition from 2D to 3D electronic structure in a particular subband of the natural superlattice of metallic atomic boron layers. At the shape resonance the electron pairs see a 2D Fermi surface at $E_F - \omega_0$ and a 3D Fermi surface at $E_F + \omega_0$, where ω_0 is the energy cut off of the pairing interaction. The resonant amplification occurs in a narrow energy range where $E_F - E_c$ is in the range of $2\omega_0$.

For further information: <http://www.superstripes.com/> and <http://www.htcs.org>

* corresponding author, email: antonio.bianconi@roma1.infn.it

PACS Codes: **74.70.Ad, 74.62.Dh; 74.80.Dm**

The material design of heterostructures is reaching the atomic limit for engineering in unprecedented ways the electronic transport [1] and optical [2] properties of materials. The electronic energy levels, wave functions and band structure of new materials can now be designed by quantum engineering. The basis of quantum engineering is the control of the quantum confinement of the electron gas in mesoscopic units to obtain artificial discrete electronic states in potential quantum wells (i.e., the classical quantum effects for a particle in a box). While in these last ten years most of the interest of the scientific community has been focused on semiconductor heterostructures, now the interest is starting to shift to metallic heterostructures in order to design and tailoring in unprecedented ways the superconducting properties [3]. The size of the mesoscopic units in these heterostructures is of the scale of the de Broglie wavelength $\lambda_F = 2\pi/k_F$ (where k_F is the wavevector of electrons at the Fermi level). While in a typical semiconductor, as gallium arsenide at room temperature, $\lambda_F \sim 250$ Å, in metallic materials due to the high charge carrier density $\lambda_F \sim 3-15$ Å. Therefore the size of the mesoscopic units in metallic heterostructures reaches the atomic limit. The thinnest possible metallic slab (also called a quantum well) is formed by atomic monolayers where the electronic charge is delocalized over an effective thickness L^* determined by the Fermi wavelength [4]. The formation of a superconducting heterostructure [5] made of a superlattice of quantum wells, B, requires a second material, A, that provides a periodic potential barrier for the electrons in the first material. The units made by the first and second material BA are repeated a large number of times to form a superlattice... BABABA... with period λ_p . A superlattice of atomic monolayers of atoms B and A, is realized by crystallographic planes of bcc or hcp, or fcc, or, honeycomb lattice of atoms A alternated with other crystallographic planes of bcc or hcp, or fcc, or honeycomb lattice of atoms A rotated one respect the others to get a crystallographic lattice matching with a lattice mismatch lower than about 8%. Therefore in the superlattice there is an

internal pressure acting on each layer of atoms (A or B) that makes stable pseudomorphic lattices of A or B that are not stable in the separated homogenous materials. The growth of artificial metallic quantum superlattices at the atomic limit has been delayed by the technical problems for epitaxial growth of thin homogenous films with sharp interfaces at the atomic limit. In fact, the metallic thin films, grown by standard evaporation methods, at this length scale get disordered on an atomic scale or granular on a mesoscopic scale and electrons get localized at low temperature.

Atomically perfect superlattices can be grown by direct chemical synthesis of elemental atoms A and B in optimized thermodynamic conditions. For example, aluminum or magnesium do not mix with boron in the solid phase and the radius of B is much smaller than the radius of Mg (Al). However they can form a heterostructure with good lattice matching by forming honeycomb graphite-like boron monolayers alternated with hexagonal, A=Mg, Al, monolayers as shown in Fig. 1, that is known as a AIB_2 crystallographic structure [7-10].

According with a recent patent the superconducting properties can be tailored and the superconducting temperature amplified by a large factor in a superlattice of quantum wells by tuning the chemical potential at a "shape resonance" for the superconducting gap [11-22], This "shape resonance" was first observed in the natural superlattice of quantum stripes (called superstripes) in a cuprate perovskites, where by changing the charge density the chemical potential is tuned to a particular quantum critical point (QCP) of the electronic structure where the "shape resonance" occurs and the superconducting critical temperature is amplified from the standard low temperature range (from millikelvin to about 10 kelvin) to the high temperature range 40-150K. This very large amplification of the superconducting gap and the critical temperature can be calculated with the BCS approach to be of the order of 100-1000 times. The quantum critical point that gives the superconducting shape resonance is a point at energy E_c in the electronic band structure of the superlattice where

there is a dimensional 2D-3D transition by moving the chemical potential through E_c as shown in Fig. 2. The superlattice has i) a 2D (or 1D for stripes) electronic structure in the energy range at $E < E_c$ for a hole-like band where hopping between the metallic units in the transversal direction is not allowed and ii) a 3D (or 2D for stripes) electronic structure in the energy range at $E_c < E < E_0$ (see Fig. 2) for a hole-like band, where hopping between the metallic units in the transversal direction is allowed.

The shape resonance for the superconducting gap occurs where the chemical potential is tuned in the range $|E_F - E_c| \sim \omega_0$ where ω_0 is the energy cut off for the pairing interaction in the generalized BCS equation, that determines the width of the superconducting shape resonance. The shape resonance can be reached by changing both the charge density that controls the position of E_F and/or the lattice parameters of the superlattice that control the energy position of E_c and E_0 . The difficulty to reach the resonating point is due to the fact that the resonance is very narrow and the charge density need to be controlled in a very fine scale in order to move the chemical potential in the energy scale of $\omega_0 \ll E_F$ in good metals. On the other hand the spacing and the periodicity of the metallic monolayers need to be controlled in the picometer scale in order to move the position of the quantum critical point E_c in the range of $-\omega_0$.

Recently Akimitsu and its collaborators [24] have discovered that MgB_2 shows high T_c superconductivity with a BCS like behavior [25,26] while similar intermetallics show only very low T_c . It has been shown that the high T_c occurs at a specific quantum critical point (QCP) [27] defined by critical values of the lattice parameters a_c and c_c and charge density ρ_c . It has been showed that by moving out from this QCP by adding dopants [28] or pressure [29] the critical temperature decreases.

Here we report an investigation of the high T_c phase in MgB_2 by a fine tuning of both the charge density and superlattice parameters a and c by aluminum doping. We show that the chemical potential is well tuned at the superconducting shape resonance and T_c decreases by very small deviation out of the critical point.

The powder $Mg_{1-x}Al_xB_2$ samples have been synthesized by direct reaction of the elements. The starting materials were elemental magnesium and aluminum (rod, 99.9 mass% nominal purity) and boron (99.5 % pure <60 mesh powder). The elements in a stoichiometric ratio were enclosed in tantalum crucibles sealed by arc welding under argon atmosphere. The Ta crucibles were then sealed in heavy iron cylinder and heated for one hour at 800 °C and two hours at 950 °C in a furnace. The samples were characterized by x-ray diffraction (XRD) in a Philips system using $Cu K_\alpha$ radiation and the lattice parameters were determined at room temperature

The Al dopants in different $Mg_{1-x}Al_xB_2$ samples control 1) the spacing and periodicity between the metallic boron layers as measured by the change of the c -axis, 2) the B-B distance as measured by the a -axis and they increase the charge density of x electrons per unit cell. In Fig. 4 we report the variation of the 002 diffraction line probing the spacing of the boron monolayers as shown in Fig.1. By increasing Al content we observe a contraction of the spacing between the metallic layers. The variation of the ratio c/c_0 where c_0 is the crystallographic axis in undoped MgB_2 compound is plotted in Fig. 5. The contraction follows the expected variation of a solid solution of AlB_2 and MgB_2 indicated by the solid line with a 0.8% variation at 8% doping, and we show that it is possible to control the material design of a superlattice of quantum wells at the atomic limit by chemical doping with a precision better than 0.3 picometers. Fig. 5 shows that the variation of the a -axis with low aluminum doping is much smaller than that of the a axis as expected [28, 29].

The superconducting properties of $Mg_{1-x}Al_xB_2$ superconductors have been investigated by the temperature dependence of the complex conductivity by the single-coil inductance method [30]. This method is based on the influence of the sample on the complex radio frequency impedance of a LC circuit shown on the insert of Fig. 6. Temperature-dependent measurements of the complex impedance, with and without the sample, allow to extract the complex

conductivity of the sample. The real part of the complex conductivity is related with the dissipative conductivity, while the imaginary part is a measure of the London penetration depth. Therefore, the temperature dependence of the imaginary part contains information about the superfluid density and dissipation effects in the vortex dynamics. Fig. 6 shows the ratio of the square of resonant frequencies $\frac{f_0(T)^2}{f(T)^2}$ where, $f(T)$, and $f_0(T)$ are the resonance frequency measured without and with the sample located in the vicinity of the coil. A sketch of the experimental circuit geometry is shown as an inset to the figure. Due to superconducting transition, the inductance L of the circuit decreases because of the screening sheet currents, and, hence, the resonant frequency $f(T)$ shows a sharp increase and therefore a sharp drop of the ratio $\frac{f_0(T)^2}{f(T)^2}$ below the transition temperature T_c is visible. The maximum of the derivative $\frac{f_0(T)^2}{f(T)^2}$ has been used to define T_c as it is shown in the upper panel of Fig. 6. The results show that we have succeeded by aluminum doping to change at the same time two key parameters that control the critical temperature:

- 1) the charge density has been changed from 8 electrons/cell to 8.08 electrons/cell and therefore we have realized a fine tuning of the chemical potential
- 2) the lattice parameter c has been changed by 0.8% and the a -axis by 0.1% in order to move the energy position of both E_0 and E_c in the band structure, where E_0 is the top of the σ -band at the A point and E_c is the critical point for the 2D->3D transition at the Γ point of the band structure [31-33].

Finally in Fig. 7 we report the variation of the critical temperature as a function of the energy shift $\Delta(x)$ of the energy difference between the Fermi level, E_F , and the position of the QCP at E_c determined by the joint variation of the charge density and the lattice parameters. By increasing x both E_F and E_c

increase but their difference Δ increases by only about 100 meV going from pure MgB_2 to the aluminum content $x=8\%$. A simple fit with a parabolic function shows that high T_c appears in a narrow energy range of the order of hundred meV i.e. two times $\omega_0=80$ meV (the energy cut off for the pairing interaction in MgB_2) convoluted with the energy dispersion in the c-axis direction as it is expected for a superconducting "shape resonance".

In conclusion we have found that the critical temperature is very sensitive to small variations of the relative position of E_F from E_c in the energy range smaller than ω_0 , that is the specific feature of a shape resonance. Further work is going on at higher Al doping to investigate the actual shape of the shape resonance shown in Fig. 7 with quantitative comparison with band structure calculations of Al doped crystals. The MgB_2 system provides a material where it is possible to modulate the spatial and electronic structure of a superlattice of metallic quantum wells at the atomic limit. It becomes now feasible to design new heterostructures at the atomic limit to be synthesized by chemical reactions to reach higher T_c approaching room temperature.

We would like to thank A. Perali, J. B. Neaton and S. Massidda for useful discussions and information on the relative shift of E_c and E_F in the electronic band structure with aluminum doping. This research has been supported by i) Progetto 5% Superconduttivit del Consiglio Nazionale delle Ricerche (CNR); ii) Istituto Nazionale di Fisica della Materia (INFM); and iii) the "Ministero dell'Universit e della Ricerca Scientifica (MURST).

REFERENCES

1. S. Datta *Electronic Transport in Mesoscopic Systems* (Cambridge University, Cambridge, 1996).
2. F. Capasso, J. Faist, and C. Sirtori *J. Math. Phys.* **37**, 4775 (1996).
3. M. Brooks, *New Scientist* No.2192, 38, 26 Jun1999; A. Bianconi *Physics World* 11, N0.7 pag. 20 (July 1998)
4. I. P. Batra S. Ciraci, G.P. Scrivastava J.S. Nelson, and C.Y. Fong *Phys. Rev. B* **34**, 8246 (1986); S. Ciraci and I. P. Batra *Phys. Rev. B* **33**, 4294 (1986).
5. S. T. Ruggiero and M.P. Beasley in *Synthetic Modulated Structures* edited by L. L. Chang and B.C. Giessen, New York Academic Press (1985) pag. 365.
6. F. J. Himpsel, *Phys. Rev B* 44, 5966 (1991); J. E. Ortega, F. J. Himpsel G. L. Mankey, and R. F. Willis *Phys. Rev. B* 47, 1540 (1993); G. L. Mankey, R. F. Willis and F.J. Himpsel, *Phys. Rev. B* 47, 190 (1993); P. Segovia, E. G. Michel and J.E. Ortega, *Phys. Rev. Lett.* **77**, 3455 (1996).
7. W. Hoffmann and W. J nicke *Naturwiss.* **23**, 851 (1935); *Z. Physik. Chem.* **31 B**, 214 (1936).
8. V. Russel, R. Hirst, F. Kanda, and A. King *Acta Cryst.* **6**. 870 (1953).
9. E. Jones and B. Marsh *J. Am. Chem. Soc.* **76**, 1434 (1954).
10. P. Duhart *Ann. Chim. t.7*, 339 (1962).
11. European Patent N. 0733271 "*High T_C superconductors made by metal heterostuctures at the atomic limit*"; (priority date 7 Dec 1993), published in *European Patent Bulletin* 98/22, 1998. see the web site <http://www.superstripes.com/>.
12. A. Bianconi *Sol. State Commun.* **89**, 933 (1994).
13. A. Bianconi, M. Missori, N. L. Saini, H. Oyanagi, H. Yamaguchi, D. H. Ha, and Y. Nishiara *Journal of Superconductivity* **8**, 545 (1995).
14. A. Perali, A. Bianconi, A. Lanzara, and N. L. Saini *Solid State Communications* **100**, 181 (1996).

15. A. Perali, A. Valletta, G. Bardelloni, A. Bianconi, A. Lanzara, N.L. Saini *J. Superconductivity* **10**, 355-359 (1997) (Proc. of the First Inter. Conference on *Stripes, Lattice instabilities and high T_c Superconductivity* Roma Dec 1996).
16. A. Valletta, G. Bardelloni, M. Brunelli, A. Lanzara, A. Bianconi, N.L. Saini *J. Superconductivity* **10**, 383-387 (1997), (Proc. of the First Inter. Conference on *Stripes and high T_c Superconductivity* Roma Dec 1996).
17. A. Bianconi, A. Valletta, A. Perali, and N.L. Saini *Solid State Commun.* **102**, 369 (1997).
18. A. Valletta, A. Bianconi, A. Perali, N. L. Saini *Zeitschrift fur Physik B* **104**, 707 (1997).
19. A. Bianconi, A. Valletta, A. Perali, and N. L. Saini *Physica C* **296**, 269 (1998).
20. A. Bianconi, S. Agrestini, G. Bianconi, D. Di Castro, N. L. Saini, in *Stripes and Related Phenomena*, A. Bianconi N. L. Saini Editors, Kluwer Academic/Plenum publisher, New York, 2000 p. 9-25 (Proc. of the second Int. Conference on *Stripes and high T_c Superconductivity* Roma Jun 1998).
21. A. Bianconi *Int. J. Mod. Phys. B*, **14**, 3289-3297 (2000) (Proc. of the third Inter. Conference on *Stripes and high T_c Superconductivity* Roma Sept 2000).
22. N. L. Saini and A. Bianconi *Int. J. Mod. Phys. B*, **14** 3649-3655 (2000) (Proc. of the third Int. Conference on *Stripes and high T_c Superconductivity* Roma Sept 2000).
23. A. Bianconi, G. Bianconi, S. Caprara, D. Di Castro, H Oyanagi, N. L. Saini, *J. Phys.: Condens. Matter*, **12** 10655 (2000).
24. J. Nagamatsu, N. Nakagawa, T. Muranaka, Y. Zenitani, and J. Akimitsu, *Nature* **410**, 63 (2001)
25. S. L. Bud'ko, S. L. Lapertot, C. Petrovic, C. E. Cunningham, N. Anderson, and P. C. Canfield; cond-mat/0101463 (2001)
26. D. E. Finnemore, J. E. Ostenson, S. L. Bud'ko, G. Lapertot, and P. C. Canfield; cond-mat/0102114 (2001).
27. A. Bianconi, N. L. Saini D. Di Castro, S. Agrestini, G. Campi, A. Saccone, S. De Negri, M. Giovannini, M. Colapietro. cond-mat / 0102410 (2001).

28. J. S. Slusky, N. Rogado, K. W. Reagan, M. A. Hayward, P. Khalifah, T. He, K. Inumaru, S. Loureiro, M. K. Hass, H. W. Zandbergen, R. J. Cava; cond-mat/ 0102262 (2001).
29. J. D. Jorgensen, D. G. Hinks, and S. Shortl cond-mat/ 0103069 (2001).
30. D. Di Castro, N.L. Saini, A. Bianconi, A. Lanzara *Physica C* **332**, 405 (2000).
31. J. Kortus, I. I. Mazin, K. D. Belashchenko, V. P. Antropov, and L. L. Boyer; cond-mat/0101446 (2001).
32. G. Satta, G. Profeta, F. Bernardini, A. Continenza, S. Massidda; cond-mat/0102358 (2001).
33. J. M. An and W. E. Pickett; cond-mat/0102391 (2001).

Figure Captions

Fig. 1. Pictorial view of the superlattice of metallic boron monolayers (B) made of graphite-like honeycomb lattice separated by hexagonal Mg layers (A) forming a superlattice ABAB in the c-axis.

Fig. 2. The quantum critical point at energy E_c at the top of a single particular subband of the electronic structure of a superlattice of quantum wells (stripes) where the partial electronic structure of this subband shows a dimensional transition from $(n-1)D$ at $E < E_c$ to nD in the range $E_c < E < E_0$ ($n=3$ for a superlattice of quantum wells and $n=2$ for a superlattice of quantum stripes). The superconducting gap shows the "shape resonance" where the pairing interaction involves pairing of nD states at $E_F + \omega_0$ and $(n-1)D$ states at $E_F - \omega_0$ for hole like subbands.

Fig. 3. Pictorial view of the transition from a 2D-like Fermi surface for a particular subband of a superlattice of quantum wells, if the chemical potential is lower than E_c to a 3D-like Fermi above E_c . The shape resonance for the superconducting gap occurs where $E_F - \omega_0$ is below and $E_F + \omega_0$ above E_c .

Fig. 4. The (002) diffraction line recorded using the Cu $K\alpha$ radiation, probing the contraction of the c-axis with Al doping in $Mg_{1-x}Al_xB_2$ samples with $x=0, 2\%, 4\%$ and 8% .

Fig. 5. The variation of the ratio a and c axis: $a(x)/a_0$ and $c(x)/c_0$ as a function of Al doping x (where a_0 and c_0 are the crystallographic axis in undoped MgB_2 compound) in $Mg_{1-x}Al_xB_2$ samples with $x=0, 2\%, 4\%$ and 8% .

Fig. 6. The variation of the critical temperature in $\text{Mg}_{1-x}\text{Al}_x\text{B}_2$ samples with $x=0, 2\%, 4\%$ and 8% . *Lower panel:* temperature dependence of the radio frequency surface resistance probed by the ratio $\frac{f_0(T)^2}{f(T)^2}$ of the resonance frequency [recorded with (f) and without (f_0) the sample] of the probing LC circuit at the superconducting transition temperature. The inset shows a cartoon sketch of the geometry of the experimental circuit used for the measurements. *Upper panel:* the derivative of the ratio $\frac{f_0(T)^2}{f(T)^2}$ probing the surface resistance, shows a peak used here to define T_c as a function of doping.

Fig. 7 Variation of the critical temperature as a function of the energy separation Δ between the Fermi level E_F and the quantum critical point, E_c defined in Fig. 2. We have taken $\Delta=0$ for the pure MgB_2 and the energy shift of E_c has been estimated from the variation of the lattice parameters and normalized at $\Delta_0=80$ meV.

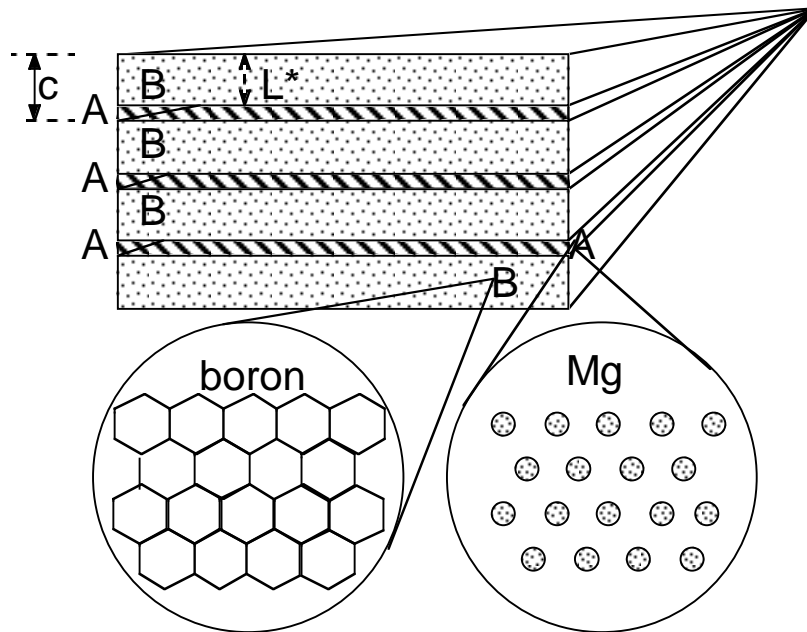


Fig. 1

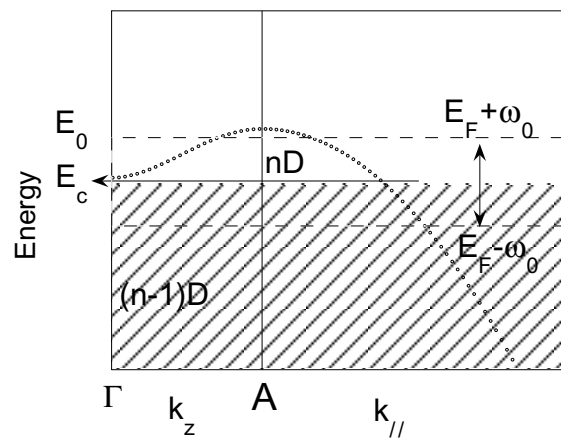


Fig. 2

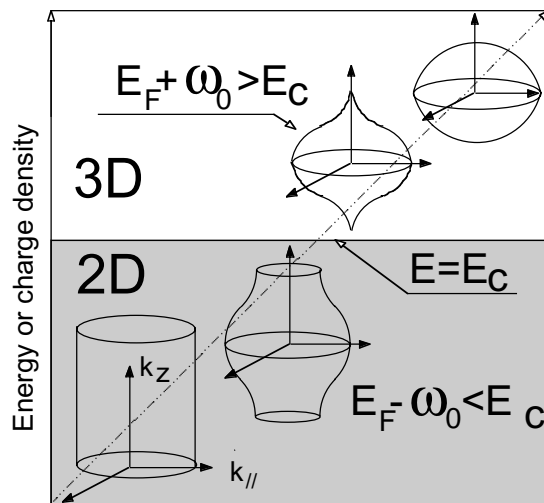


Fig. 3

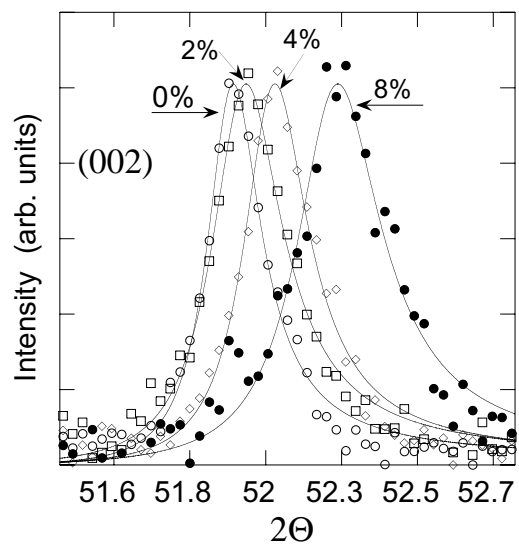


Fig. 4

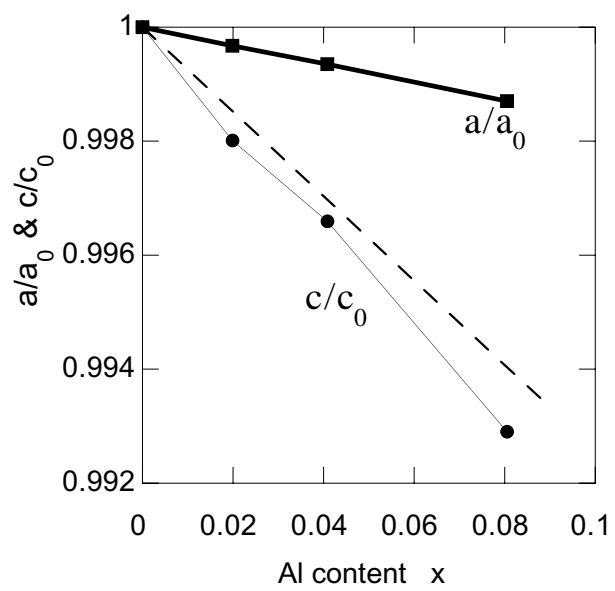


Fig. 5

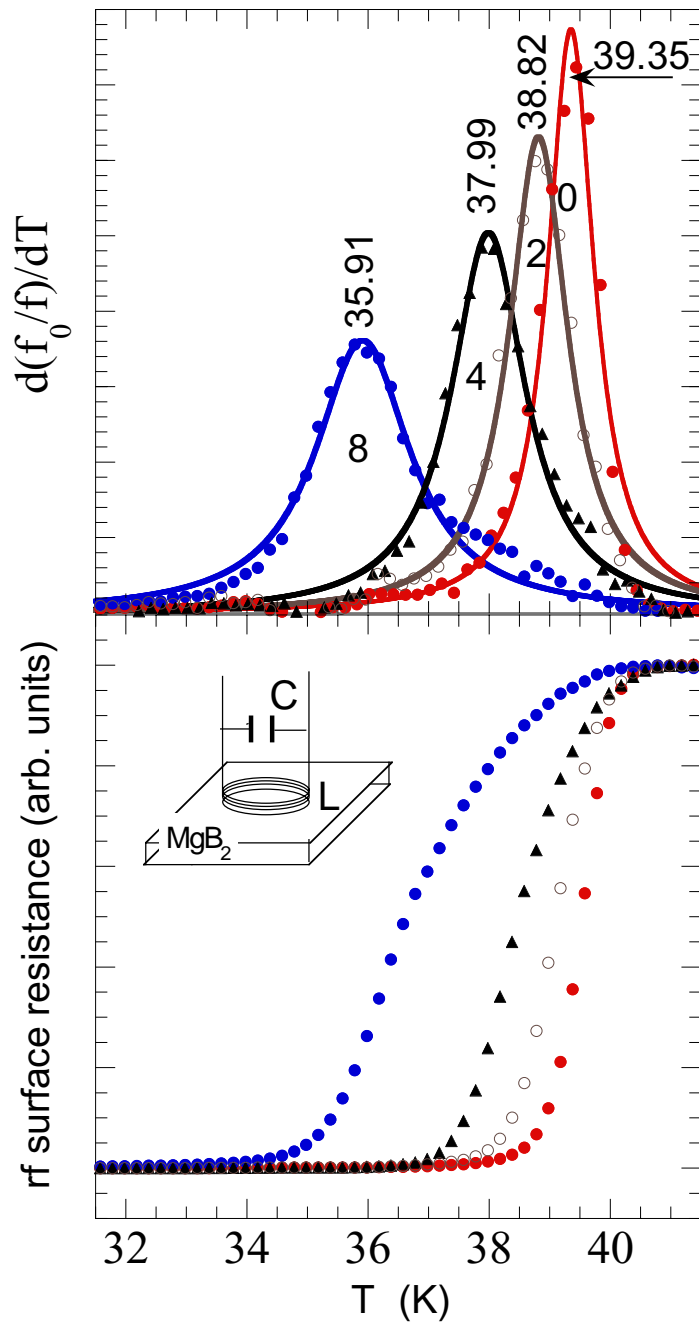


Fig. 6

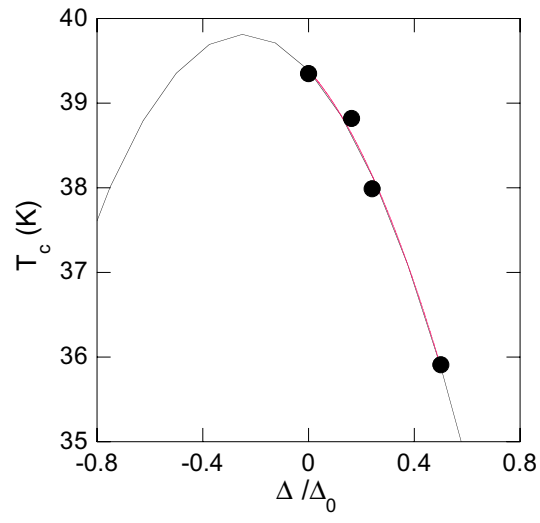


Fig. 7